Lynn M. Neitzey
M. Shane Hutson
George Holzwarth

Department of Physics,
Wake Forest University,
Winston-Salem, NC

Two-dimensional motion of DNA bands during 120° pulsed-field gel electrophoresis

The position and velocity of a band of double-stranded, linear DNA from bacteriophage G were measured during 120° pulsed-field gel electrophoresis, using a video micrometer. Both the x and y coordinates were determined simultaneously in the plane of a 1% agarose gel; x is the mean drift direction. For pulse durations T greater than the tube renewal time T^*, the path traced by the band of 670 kb DNA in the xy plane was in remarkably good accord with that predicted by Southern's ratchet model. However, the measured instantaneous velocity v_x showed a sharp backward spike each time the field changed direction, with amplitude about twice the mean drift velocity. This spike is not consistent with models which assume a constant curvilinear velocity of DNA in a tube, nor with the biased reptation model without fluctuations. The corresponding measurements of v_y showed a sharp positive spike with amplitude more than 3 times the plateau velocity in the y direction; neither model predicted this. The sharp velocity spikes are consistent with the idea that, for $T > T^*$, a large fraction of the DNA chains are stretched into U-shaped or herniated configurations. When the field changes direction, the arms of the U's and the hernias recoil rapidly in response to intramolecular DNA chain tension. Because the base of a U or hernia is fixed by gel fibers, the center of mass of the chain recoils backward every time the field changes direction.

1 Introduction

Pulsed-field gel electrophoresis (PFGE) of DNA is now a routine protocol for the separation of megabase DNA [1]. However, at the molecular level, there are still many unanswered questions about how the DNA moves from the well to its final position in the gel [2–4]. In this paper we report measurements of the instantaneous two-dimensional position (x, y) of a band of fluorescently stained G DNA in an agarose gel while the field was switched back and forth by 120° in the plane of the gel, as in the contour-clamped homogeneous electric field (CHEF) method [5, 6]; the x coordinate is the mean drift direction along the bisector of the two fields (Fig. 1). The measurement of x and y was repeated every 0.4 s with a video micrometer. From the measured x and y coordinates, the velocities $v_x(t)$ and $v_y(t)$ were determined. Our goal in these experiments was to elucidate the molecular motions which, when integrated with respect to t, lead to the observed separations.

In a previous study with the video micrometer, it was shown that T4, G, and *S. pombe* DNA exhibit a complicated velocity response immediately after a one-dimensional field is applied to a gel [7]. If the pulse is preceded by a pulse of opposite sign, as in field inversion, the DNA shows a large velocity spike immediately after the field is applied. It was also found that DNA bands recoil over substantial distances when the elctrophoretic field is turned off [7]. The most probable molecular origin for both these observations is that a large fraction of the DNA molecules in a gel is in U-shaped or herniated configuration when the DNA is driven through the gel by a field. Such configurations are among the most common configurations observed in video micrographs of single DNA chains during electrophoresis [8–13]; they are also a prominent feature of computer simulations which permit tube length fluctuations and tube leakage [14–19]. Such simulations have been quite successful in reproducing the instantaneous velocity and the oscillations in alignment which occur during field inversion [15, 17–19]. When the field is turned off or changes sign, chain tension will cause the center of mass (CM) of U-shaped chains to recoil toward the base of the U a distance of order 0.25 times the contour length. Molecules with hernias will also recoil, but for a lesser scaled distance, in a direction opposite to that in which the herniated structure was established, because the origin of the hernia is fixed by gel fibers, whereas the leading tip is free to retract.

Although 120° PFGE is perhaps the most commonly used variant of PFGE, our understanding of it is less complete than that of field-inversion gel electrophoresis (FIGE). Only a few video micrographs have been published for 120° changes in field direction [20]. Measurements of the alignment of DNA during 120° PFGE show a complex, oscillatory response when the field changes direction [21, 22]. Simulations in which the field switches by 120° have been presented for the biased reptation model (BRM) without tube length fluctuations [23] and with tube length fluctuations but not hernias [24]; a Monte Carlo procedure which permits long-range hopping of slack in the chain has also been applied to 120° PFGE [16]. The BRM with fluctuations has met with some success in predicting the dependence of average mobility on chain length and pulse time. The modified Monte Carlo simulation, in which hernias play an increasingly important role as the molecular weight of the chain increases, has been quite successful in predicting the dependence of average mobility on molecular weight, pulse duration, and field angle [16]. However, the average mobility, which is the only experimental outcome reported in most PFGE studies, is the net result of a complicated, time-dependent process. Comparisons between measurements

Correspondence: Dr. G. Holzwarth, Department of Physics, Wake Forest University, P. O. Box 7507, Reynolda Station, Winston-Salem, NC 27109, USA

Abbreviations: BRM, biased-reptation model; **CHEF,** contour-clamped homogeneous electric field (electrophoresis); **CM,** center of mass; **FIGE,** field-inversion gel electrophoresis; **kb,** kilobasepairs; **PFGE,** pulsed-field gel electrophoresis

0173-0835/93/0404-0296 $5.00+.25/0

of the instantaneous velocity and simulations should be more incisive tests of the validity of different models. In the above discussion and in all the simulations, it is assumed that the agarose matrix can be adequately represented by a static array of obstacles or pores. There is evidence that the agarose moves during PFGE [25–28], but the importance of these motions to PFGE separations remains controversial.

2 Materials and methods

2.1 DNA, gels and buffer

Buffer was 0.5 × TBE (45 mM Tris base, 45 mM boric acid, 1.25 mM EDTA, pH 8.3) Gels were prepared with 1% agarose having endosmosis 0.10–0.15 (FMC SeaKem, LE grade). Agarose was mixed with buffer, heated in a microwave oven for 5 min at 100 °C, filtered through a 0.6 μm filter to improve optical clarity, cast in trays heated to 50 °C, then left to age overnight at room temperature. Wells were arranged in pairs, called Band 1 and Band 2, forming a 90° V pattern, as shown in Fig. 1. The V was oriented so that its bisector was parallel to the mean drift direction, labeled x in Fig. 1. Band 1 was used to track DNA motion at +45° to x whereas Band 2 was used to track DNA motion at −45° to x. For reasons discussed in Section 2.3, this procedure gave much better precision in two dimensions than could be obtained from a single band. Wells were 1 mm wide, 5 mm long, and approximately 3 mm deep; three such V's were present in a single gel, allowing three experiments. DNA from bacteriophage G was released from the phage (Carolina Biological Supply Co.) by adding "sodium dodecyl sulfate (SDS) dye mix" [29], heating for 10 min at 65 °C, then cooling to 0 °C. The size of G DNA, based upon its electrophoretic mobility relative to the chromosomes of the yeast *S. cereviseae*, is 670 kb. About 15 μL were placed in each well. Gels containing DNA were prepared in a two-step procedure. First, the DNA was run into the gel with a 0.75 V/cm DC field for 30 min. This was followed by 4 h at 4 V/cm in a Bio-Rad CHEF II system with a pulse ramp from 100 to 300 s to ensure that bands contained only undegraded G DNA. During this time, the net displacement of the DNA from the wells was about 1 cm. After the prerun, the gel was stained with 0.1 μg/mL ethidium bromide (EB), destained in 0.5 × TBE, and photographed on a 300 nm transilluminator. The bands retained the V shape of the wells without distortion as they drifted in the x direction.

2.2 Electrophoresis chamber and field electronics

A chamber was designed to provide fields E_A and E_B directed at 120° to one another (Fig. 1). The field E_A was generated by 16 platinum wires arranged in 2 parallel lines of 8 electrodes each; the ends of the lines curved inward to reduce fringing. The field E_B was generated by a second set of 16 electrodes. The gel was located midway between each pair of parallel lines. Field homogeneity and direction were determined by mapping the potential in the assembled chamber; the angle between E_A and E_B was 116 ± 3°. Buffer was recirculated at 300 mL/min and cooled to 10 °C by an external heat exchanger. The amplitude and period of the potential differences V_A and V_B applied to the electrodes were controlled by a Keithley ATE 150 programmable power supply and mercury-wetted reed relays under IEEE-488 bus control. An important feature of the design, which is not possible with diode-based CHEF systems, was that the fields were reversible; this permitted us to restore the bands to their original locations.

2.3 Video micrometer

The positions of the two arms of a V-shaped band of fluorescently labeled DNA in a gel were determined by illuminating the V from below with light from an argon-ion laser and observing the fluorescent image from above with a video camera. The instrument has been described previously [7]. The laser (Ion Laser Technologies Model 5500A) produced 50–200 mW of light with $457.9 < \lambda < 514.5$ nm. A 10 × beam expander enlarged the beam to illuminate a 2-cm-diameter region of the gel. An OG 570 glass absorption filter, placed just in front of the camera lens, blocked scattered laser light while transmitting fluorescent light from the DNA band ($570 < \lambda < 630$ nm) to the camera. The camera was a Hamamatsu C2400 model fitted with Newvicon sensor, Canon 50 mm f/1.4 collecting optics, and 50 mm extension tube. The gel, electric fields, and camera axes (x_c, y_c) were aligned as shown in Fig. 1. The RS-170 video signal from the camera was digitized to 8-bit precision and processed by an image processing board (Image 1280, Matrox Electronic Systems, Quebec, Canada). Four frames were summed to reduce noise. Band position was determined to subpixel precision by an intensity-weighted centroid algorithm: $< i > = \Sigma_{ij}\, iI_{ij}/\Sigma I_{ij}$, $< j > = \Sigma_{ij}\, jI_{ij}/\Sigma I_{ij}$, where i is column number, j is the row number, and I_{ij} is the light intensity at that pixel. Values of both $< i >$ and $< j >$ were determined for both Band 1 and Band 2. However, the precision of $< i >$ for Band 2 and $< j >$ for Band 1, about ± 0.02 pixel in favorable cases, were about 10 times superior to the precision of $< j >$ for Band 2 and $< i >$ for Band 1. The reason

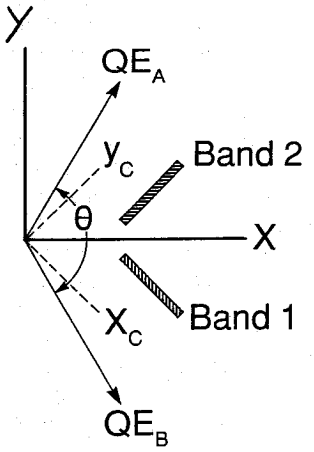

Figure 1. Coordinate system of the video micrometer. QE_A and QE_B show the directions of the electric forces which were applied alternately to the DNA; the angle between E_A and E_B is 120° and is labeled θ. The mean drift of the DNA was along the bisector of E_A and E_B, which is labeled as x; y is perpendicular to x. The camera was oriented at 45° to the $[x,y]$ coordinate system; the camera rows and columns are labeled by x_c and y_c, respectively. Two wells, labeled as Band 1 and Band 2, were used for each experiment, to improve precision. The two bands were arranged at 90° to one another and were oriented parallel to x_c and y_c, respectively.

for this is that a small displacement perpendicular to a band affects the intensity of many pixels along the entire length of the band, whereas a similar small displacement along the long axis of a band affects only the much smaller number of pixels at either end of the band. The more precise values of $< i >$ and $< j >$ were used to specify the position of a V. The conversion factors between image location in pixels at the camera and band position (x_c, y_c) in μm were determined by placing a steel scale at the object plane of the detector and counting the number of pixels between marks on the image of the scale: $x_c = 25.1 < i >$ μm, $y_c = 19.6 < j >$ μm.

2.4 Data analysis

Band position in the more conventional coordinates (x, y), with x parallel to the mean drift direction (along the median between E_A and E_B) and y describing motion at right angles to the mean drift velocity, were computed by standard formulas: $x = x_c \cos\alpha + y_c \sin\alpha$, $y = -x_c \sin\alpha + y_c \cos\alpha$, where α is the angle between x and x_c; in our chamber $\alpha = 45°$. The velocity components v_x and v_y were computed by differentiating $x(t)$ or $y(t)$ with respect to t, using a Savitzky-Golay [30] 7-point smoothing algorithm provided in the AXUM software package (Trimetrix, Seattle, WA).

3 Results

3.1 *x vs. y* for various pulse periods

The band position (x,y) was measured during PFGE for pulse periods T ranging from 5 to 260 s. These pulse periods span the PFGE "antiresonance" or mobility minimum which, for G DNA, occurs at $T = 75$ s when $E = 4$ V/cm. Experimental results for 2 complete cycles, E_A, E_B, E_A, E_B at each of 4 representative pulse periods, $T = 200$, 121, 63, and 13 s, are shown in Fig. 2 A–D. Figure 2 E–G are calculated results for a simple model which will be discussed only after the experimental observations have been presented. For $T = 200$ s (Fig. 2 A), the DNA spent most of the time drifting in a straight line in the direction of the field. However, just after E changed direction, the DNA partially retraced the path defined during the previous pulse. The total distance travelled in the drift direction (x) during one cycle (2 pulses) was 140 μm, but during that time the band twice ratcheted backward 9 μm in the $-x$ direction. In the meantime, it travelled 163 μm in the $+y$ direction, then back the same distance on the opposite pulse. The net result was a displacement of 140 μm in 400 s, giving an average velocity of 0.35 μm/s.

For shorter T, the DNA spent a larger fraction of the time moving backward in the $-x$ direction, as shown in Fig. 2 B for $T = 121$ s. The distance travelled in the $-x$ direction every time the field changed direction was 10 μm, which was almost unchanged from the results at 200 s. However, less time remained for travel in the $+x$ direction, so that the net drift in the $+x$ direction for 1 complete cycle was only 54 μm. Meanwhile, the motion in the y direction was ± 98 μm. The net result was a reduced average velocity: 54 μm/242 s = 0.22 μm/s. For $T = 63$ s, the band never moved truly parallel to the electric field (Fig. 2 C). It moved about 6 μm in the $-x$ direction every time the field changed direction, then advanced 12.5 μm in the $+x$ direction. Meanwhile, the excursions in y direction remained large, ± 62 μm. The average velocity was only 12.5 μm/126 s = 0.10 μm/s. For $T = 13$ s, which was much less than the "antiresonance" period, the band moved less than 1 μm in the $-x$ direction each time the field switched, then advanced about 2.5 μm (Fig. 2 D). The angle between displacements during alternate pulses was far from 120°. Displacements in the y direction were only ± 18 μm. The average velocity in the x direction was 3.75 μm/26 s = 0.14 μm/s.

The ratchet model for 120 ° PFGE, in the simple form first described by Southern [31], provides a framework for discussing these results, especially for longer pulse durations, despite its limitations. In this model, the DNA is assumed to be stretched to an invariant length L, which is a fraction of the contour length L_c. The gel provides a "tight tube" in which the DNA chain moves at constant curvilinear velocity v. The leading end or head always moves in the direction of QE, where Q is the charge on the chain. When the field switches direction by an angle greater than 90°, as is the case in our experiments, the two ends of the chain alternate in the role of leading segment. Because of the "tight tube" assumption, the chain retraces the last segment of path, of length L, laid down in the preceding pulse, giving the effect of a ratchet. As shown in the Appendix (Section 6.1), the average velocity $< v_x >$ of the CM, along the x-direction, is

$$< v_x > = [v - (L/T)] \cos(\theta/2) \quad (1)$$

For long T, this simple equation predicts in a qualitatively correct manner the dependence of $< v_x >$ on T and L. For $T < L/v$, the model predicts that $< v_x > = 0$ because the chains oscillate about the pivot point of the ratchet, whereas experiment shows that v_x does not go to zero at T^* and in fact increases with decreasing T for $T < T^*$. The model is nevertheless useful here because it incorporates the simplest geometrical aspects of 120° PFGE, the ratchet behavior in which the two ends of the chain alternate in leading the chain. Deviations between our experimental results and the model will be a measure of the role of DNA recoils, tube leakage, bunching at the chain ends, or perhaps agarose motions. The model has only two parameters, v and L, which were determined by a least-squares fit of Eq. (1) to the experimental results for $< v_x >$ in the range 100–200 s: $v = 1.13$ μm/s and $L = 81.6$ μm. The effective length L is thus only 36% of the contour length of G DNA, 228 μm. The tube renewal time $T^* = L/v$ is 72.1 s.

Having fixed the 2 parameters v and L, we calculated $x(t)$ and $y(t)$ for the CM of the DNA chain, according to the model (Appendix 6.1); the results are given in Figs. 2 E–G, adjacent to the corresponding experimental curves. For $T = 200$ s, the ratchet model correctly predicted the shape of the experimental curve, including both the initial backward movement of the chain in the $-x$ direction upon each change in field direction, as well as the amplitude of the motion in the y direction (compare Figs. 2 A and 2 E). When T was changed to 121 s, the model predicted correctly the changes in the shape of the experimental curve (Fig. 2 F). Because of the shorter pulse period, the backward movement in the x direction played a larger relative role in both experiment and model. It was not possible to use the next experimental time, $T = 63$ s, because the model is invalid for

$T < T^* = 72$ s. Instead, a calculation was carried out for another pulse period very close to T^*, $T = 78$ s (Fig. 2G). The model predicted a series of almost circular arcs with large amplitude in the y direction and a tiny offset (drift) in the x direction, which was similar to the experimental observations (Fig. 2C). The model would predict no net motion for $T = 13$ s, the shortest time for which experimental data are presented. The agreement between observations and model in Fig. 2 suggests that ratchet motion is the predominant feature of the ensemble-average motions of bands of G DNA for $T > T^*$.

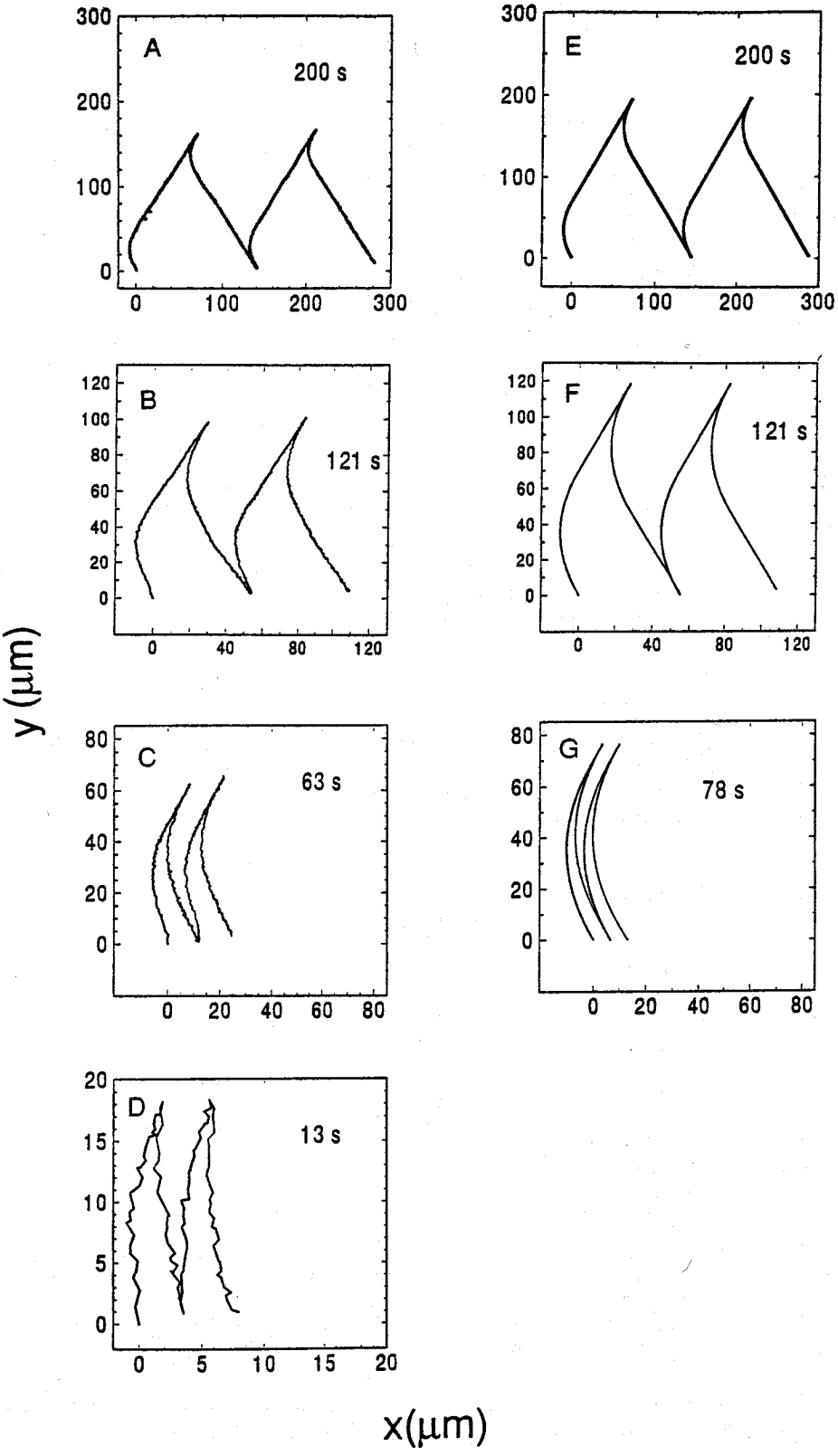

Figure 2. Plots of the position of a band of G DNA during 4 pulses of 120° PFGE (2 complete cycles) in 1% agarose with $E = 4.0$ V/cm. The first pulse was along E_A, the second was along E_B, *etc.* Panels (A)–(D) show experimental results for pulse durations $T = 200$, 121, 63, and 13 s. Panels (E)–(G) show the position computed with the ratchet model assuming constant curvilinear velocity in a tight tube (Appendix 6.1), with $T = 200$, 121, and 78 s.

3.2 Velocities v_x and v_y

The assumption of constant curvilinear v in the model is contradicted by experimental [11–13] and theoretical [14–16] evidence showing that, for chains with the size of G DNA, the velocity of individual chains fluctuates with amplitude $\pm < v >$ during gel electrophoresis as the chain conformation cycles between fairly compact, stretched, and U-shaped configurations. The ensemble average velocity of a whole band of DNA also shows large oscillations when a single pulse is applied [7]. To see whether the velocity was constant during 120° PFGE, we differentiated the meas-

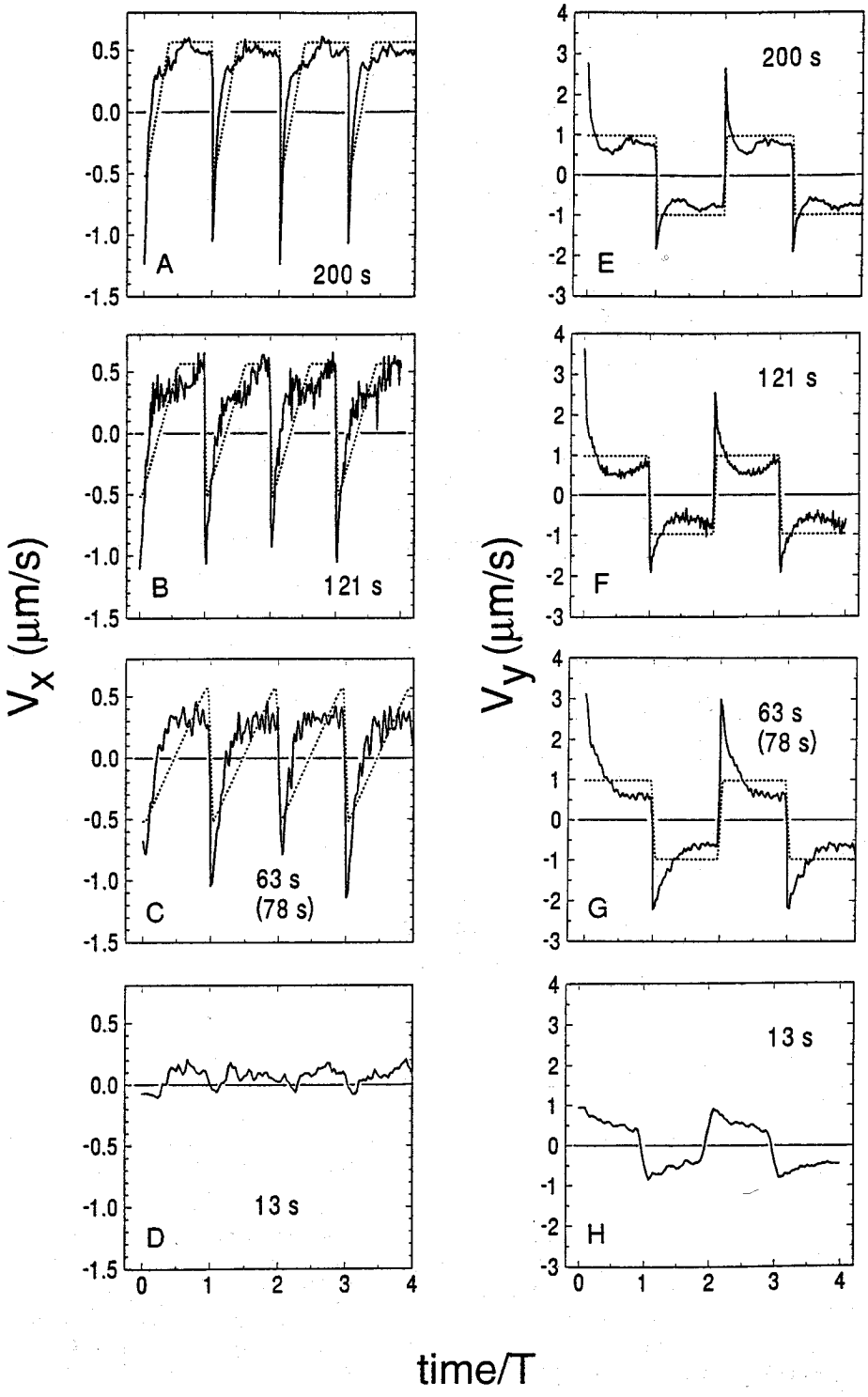

Figure 3. The velocity v_x and v_y of G DNA for pulse duration T between 200 and 13 s. Panels (A)–(D) show v_x *vs.* time, with time normalized by the period T of the pulses; the pulses alternate along the directions QE_A and QE_B. Panels (E)–(H) show corresponding v_y data. Solid lines show experimental results; dots are the predictions of the ratchet model with constant curvilinear velocity in a tight tube.

ured $x(t)$ and $y(t)$ data and plotted the resultant v_x and v_y against t. To facilitate comparisons between results for different pulse period, the t scale was normalized by T. Figures 3 A–D show the measurements for v_x. Also shown is the corresponding time-dependent v_x of the ratchet model with constant curvilinear v. For $T=200$ s, the experimental v_x had a sharp negative spike with amplitude −1.15 μm/s each time the field was switched. The velocity then increased rapidly to a shoulder of 0.35 μm/s, a peak of 0.57 μm/s at $t=100$ s, and finally a constant plateau of 0.48 μm/s until the next change in field direction. The average velocity in the x direction was large, because the molecules spent most of the period with a positive v_x. The modelled v_x showed a simpler waveshape, beginning at $-v\cos(\theta/2)=-0.565$ μm/s when $t=0$, then increasing with constant acceleration during the ratchet motion until $v_x=+v\cos(\theta/2)=0.565$ μm/s when $t=T^*=72$ s, the tube renewal time. For $t>T^*$, the model predicts that v_x is constant (Fig. 3 A).

Although the observed velocity crudely followed the model curve, large deviations were obvious. The most important difference was that the observed velocity showed a much larger and faster negative spike just after the field changed direction than did the model. This is a recoil similar to that observed recently in this laboratory for DNA subjected to unidirectional pulses [7]. The most probable molecular interpretation of the recoils is that, after the field was on for some time, a significant fraction of the DNA chains was in U conformations with the two arms of the U pointing in the direction of QE and the base of the U pinned by gel fibers. Each segment of such a U-shaped DNA chain was subject to the electrical force QE, to tension, to friction with solvent and gel fibers, and to random, Brownian forces from the solvent. The electric force and tension pulled in opposite directions and largely cancelled one another after the field had been on for some time. However, when the field was turned off or changed direction, QE and the tension no longer acted in opposite directions. Consequently, tension pulled the segments toward the base of the U, which was pinned, thus moving the center of mass backwards in a recoil. In the case of 120° PFGE, this recoil accelerated the tube renewal process every time the field changed direction. An alternative explanation for the recoils is that the chains were in what Duke and Viovy [16] call a ramified configuration, in which the chain is highly extended but has one or more hernias after being driven through the gel for many seconds. Retractions of the hernias when the field changes direction would be expected to lead to recoils of the CM.

When $T=121$ s, the experimentally observed v_x showed a negative spike of the same amplitude each time the field changed direction (Fig. 3 B). However, for this pulse period the recoil took a larger fraction of the cycle, and the velocity remained at the shoulder velocity, 0.35 μm/s, for much of the remainder of the pulse period, then reached the peak, seen at 100 s in Fig. 3 A, at the very end of the pulse, The average value of v_x during one cycle was less than for $T=200$ s because a larger fraction of the cycle was spent with negative or small positive velocity. For the model, also, a larger fraction of the pulse period was spent with negative or small positive v_x than for $T=200$ s, as tube renewal took place. For $T=63$ s, v_x looked similar to the early phases of the corresponding data for $T=200$ and 121 s, when plotted against t. When plotted against t/T, the negative spike took an even larger fraction of the pulse period, and v_x reached only the shoulder velocity, 0.32 μm/s (Fig. 3 C). The model, with $T=78$ s, barely reached the plateau, so that the integral under the curve was essentially zero ($T\approx T^*$). Finally, when $T=13$ s, the negative spikes in v_x were reduced to a mere 0.1 μm/s. The molecules had a small positive velocity, 0.15 μm/s, for about 3/4 of the period. No model curve is given; the model predicts that $v_x=0$ for $T<T^*$. The most striking difference between the experimental data for $T>T^*$ and $T<T^*$ was the absence of the negative spike for short T. This probably reflected the fact that the DNA must move a distance of order (1/4) L_c in order to fully form the U which gives the recoil. For $T=13$ s and $<v>\approx 1$ μm/s along the direction of the field, the displacement was only 13 μm, about 1/20 th of L_c.

It was shown above in the y *vs.* x plots (Figs. 2 A–D) that the DNA made great swings in the positive and negative y directions even when the actual progress of the band along x was very small. The ratchet model, in fact, predicts that $v_y(t)$ is a square wave switching between $+v\sin(\theta/2)$ and $-v\sin(\theta/2)=\pm 0.98$ μm/s whenever the field changes direction, for all $T>T^*$. The experiments showed that v_y is a more complicated function of t. For $T=200$ s, there was a sharp spike to 2.7 μm/s in the direction of QE immediately after the field changed direction, followed by a 0.5 μm/s valley, a small second peak, and then a plateau (Fig. 3 E). For $T=121$ s, the magnitude of the initial spike and the valley were almost the same as at $T=200$ s, but these features took up a larger fraction of the pulse period (Fig. 3 F). The velocity along y just about reached the second peak of 0.9 μm/s when the field was switched. For $T=63$ s, the v_y curve closely resembled the first 63 s of the data for $T=121$ and 200 s (Fig. 3 G). However, for $T=13$ s, the velocity spike was reduced to only 0.9 μm/s, followed by a gradual decline to 0.4 μm/s (Fig. 3 H). Although these values of v_y were much reduced compared to v_y for $t>T^*$, they were still large compared to v_x (Fig. 3 D).

4 Discussion

Probably the most important result of these experiments was the demonstration that DNA bands traced a ratchetlike path after each change in field direction, as Southern predicted in 1987. Any model which includes this essentially geometrical feature will therefore be at least partly successful in predicting the dependence of mobility on M and T in PFGE; details of the t-dependence of the curvilinear velocity of the DNA in its tube are irrelevant to the modelled results in Fig. 2 E–G. In particular, a constant curvilinear velocity, as assumed by Southern, was sufficient. We note that other assumptions of Southern's model, such as alternation between a unique "head" and "tail" upon field switching, as well as end-first migration, are not proven by the agreement between experiment and model (Fig. 2), because only the CM position, not the chain ends, were observed in the experiments.

Examination of the t-dependence of v_x and v_y showed that the xy plots of Fig. 2 masked a weakness of the constant-velocity model; the experiments showed that a sharp recoil occurred immediately after the field changed direction. This was not anticipated by the constant-curvilinear-velocity model. The BRM, both without and with tube-length

fluctuations [23, 24], has also been applied to 120° PFGE. In the BRM without tube length fluctuations [23], the DNA chain moves in a tight tube and advances by one end at a time. However, the electric driving force of the chain along the tube is not simply QE but rather $QE<h_x>/L$, where h_x is the end-to-end vector of the DN A. For long T, this model predicts that the chains move in the ratchet mode, with average mobility going to zero at the tube renewal time T^*. As a consequence, plots of x against y for various T will be identical to those of the simpler, constant-curvilinear-velocity model already shown in Fig. 2 E–G. The time-dependence of the velocities v_x and v_y predicted by the BRM, however, was quite different from the model with constant curvilinear velocity, and agreed poorly with experiment, as shown in Fig. 4 for $T=121$ s. The model failed to predict the sharp initial spike in both v_x and v_y every time the field changes direction. This is consistent with other failures of the BRM, such as its inability to deal with FIGE [2].

Simulations which are less restrictive than the BRM, and which include hernias, have had considerable success in predicting many features of FIGE, including the antiresonance, instantaneous velocity, and alignment. For 120° PFGE, the BRM with tube length fluctuations [24] has been fairly successful in fitting the observed average mobility, $<v_x>$, for a range of M and T. Monte Carlo simulation with long-range hopping has been even more successful in explaining the observed dependence of average mobility on M, pulse period, and field angle [16]; the chain ends dominate reorientation and ratchetlike motion occurs upon 120° reorientation. It will be interesting to see how well models can simulate the instantaneous velocities reported here.

We are grateful to the National Science Foundation for support of this research through grant DMB 8906213. We thank Louis Keiner for many helpful discussions.

Received October 2, 1992

5 References

[1] Burmeister, M. and Ulanovsky, L. (Eds.), *Pulsed-Field Gel Electrophoresis*, Humana Press, Totowa, NJ 1991, pp. 1–333.
[2] Zimm, B. H. and Levene, S. D., *Quart. Rev. Biophysics* 1992, *25*, 171–204.
[3] Viovy, J. L. and Defontaines, A. D., in: Burmeister, M. and Ulanovsky, L. (Eds.) *Pulsed-Field Gel Electrophoresis*, Humana Press, Totowa, NJ 1991, pp. 403–450.
[4] Deutsch, J. M., in: Burmeister, M. and Ulanovsky, L., *Pulsed-Field Gel Electrophoresis*, Humana Press, Totowa, NJ 1991, pp. 367–384.
[5] Chu, G., Vollrath, D. and Davis, R. W., *Science* 1986, *234*, 1582–1585.
[6] Vollrath, D., in: Burmeister, M. and Ulanovsky, L. (Eds.), *Pulsed-Field Gel Electrophoresis*, Humana Press, Totwa, NJ 1991, pp. 19–30.
[7] Keiner, L. E. and Holzwarth, G., *J. Chem. Phys.* 1992, *97*, 4476–4484.
[8] Smith, S. B., Aldrige, P. K. and Callis, J. B., *Science* 1989, *243*, 203–206.
[9] Schwartz, D. C. and Koval, M., *Nature* 1989, *338*, 520–522.
[10] Gurrieri, S., Rizzarelli, E., Beack, D. and Bustamante, C., *Biochemistry* 1990, *29*, 3396–3401.
[11] Rampino, N. J., *Biopolymers* 1991, *31*, 1009–1016.
[12] Rampino, N. J. and Chrambach, A., *Biopolymers* 1991, *31*, 1297–1307.
[13] Howard, T. and Holzwarth, G., *Biophys. J.* 1992, *63*, 1487–1492.
[14] Deutsch, J. M., *Science* 1988, *240*, 922–928.
[15] Zimm, B. H., *J. Chem. Phys.* 1991, *94*, 2187–2206.
[16] Duke, T. A. J. and Viovy, J. L., *Phys. Rev. Lett.* 1992, *68*, 542–545.
[17] Duke, T. A. J. and Viovy, J. L., *J. Chem. Phys.* 1992, *96*, 8552–8563.
[18] Deutsch, J. M., *J. Chem. Phys.* 1989, *90*, 7436–7441.
[19] Lim, H. A., Slater, G. W. and Noolandi, J., *J. Chem. Phys.* 1990, *92*, 709–721.
[20] Smith, S. B., *Individual DNA Molecules Undergoing Gel Electrophoresis* (video tape), 1988, Instructional Media Services, SB-54, University of Washington, Seattle, WA 98195.
[21] Åkerman, B. and Jonsson, M., *J. Phys. Chem.* 1990, *94*, 3828–3838.
[22] Whitcomb, R. W. and Holzwarth, G., *Nucleic Acids Res.* 1990, *18*, 6331–6337.
[23] Slater, G. W. and Noolandi, J., *Electrophoresis* 1989, *10*, 413–428.
[24] Viovy, J. L., *Electrophoresis* 1989, *10*, 429–441.
[25] Jonsson, M., Åkerman, B. and Nordén, B., *Biopolymers* 1988, *27*, 381–414.
[26] Calladine, C. R., Collis, C. M., Drew, H. R. and Mott, M. R., *J. Mol. Biol.* 1991, *221*, 981–1005.
[27] Stellwagen, J. and Stellwagen, N., *Nucleic Acids Res.* 1989, *17*, 1537–1547.
[28] Lanan, M., Shick, R. and Morris, M. D., *Biopolymers* 1991, *31*, 1095–1104.
[29] Carle, G. F., Frank, M. and Olson, M. V., *Science* 1986, *232*, 65–73.
[30] Savitzky, A. and Golay, M., *Anal. Chem.* 1964, *64*, 1627–1639.
[31] Southern, E. M., Anand, R., Brown, W. R. A. and Fletcher, D. S., *Nucleic Acids Res.* 1987, *15*, 5925–5943.

6 Appendix

6.1 The ratchet model with constant curvilinear velocity

The ratchet model for PFGE of DNA, in the form developed by Southern [31], considers the DNA chain to be a flexible rod of constant length L which moves at constant curvilinear velocity v in a "tight tube", while the field changes direction by angle θ every T seconds. Assume that the field has been cycling for some time with pulse duration $T > T^*$, the tube renewal time. At time $t=0$, when an E_A pulse begins, the molecule is initially aligned parallel to E_B because of the pulse occurring before $t=0$. If the coordinate origin is chosen such that the CM coordinates (x,y) are equal to $(0,0)$ at $t=0$, then, for $t<T^*=L/v$, x and y obey the following equations during one E_A pulse:

$$x=\left[\frac{v^2t^2}{L}-vt\right]\cos(\theta/2) \tag{2}$$

$$y=vt\sin(\theta/2) \tag{3}$$

For $t>T^*$, x and y in the model obey:

$$x=[vt-L]\cos(\theta/2) \tag{4}$$

$$y=vt\sin(\theta/2) \tag{5}$$

Consequently, although the curvilinear velocity v of the chain in its tube is constant, the CM velocities v_x and v_y are not constant. For $t<T^*$:

$$v_x=\left[\frac{2v^2t}{L}-v\right]\cos(\theta/2) \tag{6}$$

$$v_y=v\sin(\theta/2) \tag{7}$$

Fot $t>T^*$, one has

$$v_x=v\cos(\theta/2) \tag{8}$$

$$v_y=v\sin(\theta/2) \tag{9}$$

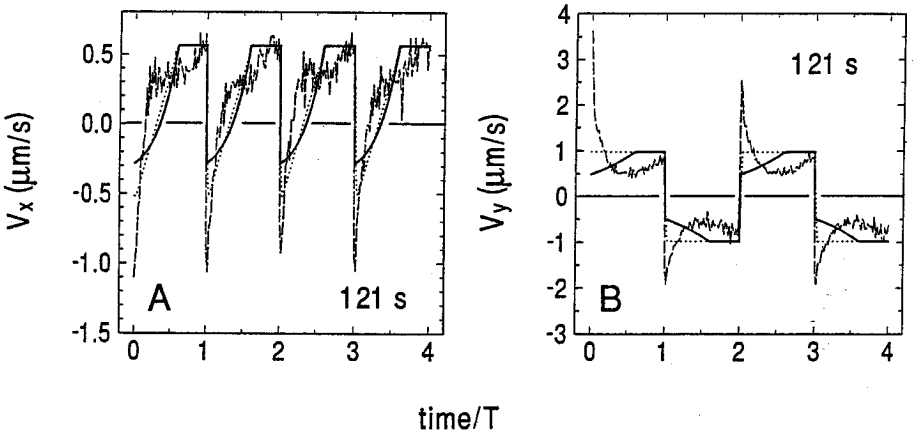

Figure 4. Modelled velocities and experimental results for $T = 121$ s. The solid line was computed from the BRM model (Appendix 6.2); dots were computed according to the constant curvilinear velocity model (Appendix 6.1); dashes show the experimental results.

6.2 BRM

The BRM was extensively explored in the early phases of modelling of PFGE. For 120° PFGE and pulse duration T greater than the tube renewal time T^*, the average mobility is predicted to vary as $1-T^*/T$, just as in the Southern model [23]. However, in the BRM, the curvilinear velocity of the DNA in its tube varies with t because the electrical force driving the chain along the tube is proportional to the projection of the chain end-to-end vector on E. Suppose $s(t)$ is the length of the new tube created after the beginning of the field E_A; the analytic form of $s(t)$ for $t < T^*$ is [23]

$$s(t) = \frac{L\cos\theta}{1-\cos\theta}\left(\exp\left[\ln\left(\frac{1}{\cos\theta}\right)\frac{t}{T^*}\right]-1\right) \quad (10)$$

For $t > T^*$,

$$s(t) = \frac{L\cos\theta}{1-\cos\theta} + v_p(t-T^*) \quad (11)$$

Here L is the length of the tube occupied by the chain. For $\theta = 120°$ and v_p equal to the plateau velocity of the chain in its tube, Eqs. (10) and (11) predict that, for $t < T^*$,

$$v_x = \frac{v_p}{2}\cos\left(\frac{\theta}{2}\right)\exp\,[0.693\ t/T^*]\,(2\ \exp[0.693\ t/T^*]-3) \quad (12)$$

$$v_y = \frac{v_p}{2}\sin\frac{\theta}{2}\ \exp[0.693\ t/T^*] \quad (13)$$

For $t > T^*$, one has

$$v_x = v_p\cos(\theta/2) \quad (14)$$

$$v_y = v_p\sin(\theta/2) \quad (15)$$

The two parameters T^* and v_p, can be determined from experimental measurements of the T-dependence of the average velocity in the x direction: $T^* = 72.1$ s and $v_p = 1.13$ μm/s in our experiments, as for the Southern model. Velocities computed for this model using these parameters are shown in Fig. 4.